Carrier Landing Simulation Using Detailed Aircraft and Landing Gear Modeling

Max McDonald,[1] Phillip W. Richards,[2] Morgan Walker,[3] and Andrew Erickson[4]
SDI Engineering Inc., Kirkland, WA, 98033, USA

Landing on an aircraft carrier is a difficult maneuver involving an aircraft, a moving carrier deck, and a complex arresting system that stops the plane in less than four seconds. Furthermore, modeling of the landing gear is difficult due to the interactions between many complicated, nonlinear subsystems. Capturing these interactions is essential to providing a realistic carrier landing simulation that can be used for pilot training and detailed landing gear design and analysis. SDI Engineering has developed GearSim, a landing gear modeling and simulation software tool, and recently adapted it for carrier landing simulations. This software program contains detailed models of all relevant landing gear subsystems, 6-DOF carrier deck motion, and a model of the aircraft arresting system. This study presents a model of the F-18 aircraft and landing gear and demonstrates the carrier landing simulation capability of GearSim.

I. Introduction

The aircraft certification process requires a significant number of flight and ground tests to ensure the aircraft's structure and landing gear perform safely under a wide range of operations. A reduction of the required number of test points in flight and ground tests could save significant cost and time during the design and analysis process, and can be achieved by using a reliable and accurate simulation capability. In addition, ground test simulations can provide improved prediction and understanding of extreme or difficult to obtain cases such as strong crosswinds, variable runway conditions, hard landings, and abrupt maneuvers.

The industry standard methods for the prediction of loads during ground operations are typically based on static force balances of the aircraft (Ref. [1]). However, dynamic effects could be included in ground loads analyses as they can lead to loads exceedances and possible fatigue issues. The ground loads analysis process can be improved with accurate modeling of landing gear dynamics, aeroelastic effects, runway conditions, wind strength and direction, and the forced displacement that drives the landing gear response. The loads during a landing condition depend on the aerodynamic conditions and approach maneuver implemented by the pilot. The touch-down velocity of the aircraft is a critical parameter in the magnitude and character of the dynamic landing loads. Crosswind conditions, turbulence, or discrete gust encounters can also influence the ground loads. Crosswind conditions can be particularly challenging to model because the approach maneuver can vary based on the personal preference of individual pilots or various operational requirements.

Carrier landings introduce new complexity and dynamics to the aircraft landing sequence: the carrier deck motion affects the tire/ground interaction and adds additional flight control complexity to the landing maneuver, and the arresting system produces large forces and moments on the aircraft after touchdown. Modeling and simulation of the carrier landing process has the potential to reduce landing gear and arresting system testing requirements and costs, and can improve the analysis of the landing gear and airframe loads for arrested landing scenarios. These models can also be integrated into existing flight simulator software programs to reduce pilot training costs. The simulations can also be used to develop enabling systems for autonomous carrier landing operations.

SDI Engineering has developed a landing gear modeling and simulation software tool based in MATLAB/Simulink called GearSim that includes aircraft models with detailed landing gear subsystems, including shock absorbers, tires, leg structures, brakes and antiskid systems. GearSim has recently been modified by adding 6-DOF carrier deck motion and a model of the aircraft tail hook and arresting gear system, and is now suitable for the

[1] Aeronautical Engineer
[2] Principal Aeronautical Engineer, AIAA Member
[3] Aeronautical Engineer Intern
[4] Principal Aeronautical Engineer, AIAA Member

simulation and analysis of arrested landing scenarios. This study has revealed that combining GearSim with models for carrier deck motion and arresting gear can accurately simulate the behavior of aircraft, landing gear, and the various subsystems during carrier landings. In the future, GearSim carrier landing results could be integrated into a flight simulator environment that would improve simulation accuracy and serve as an excellent tool to train pilots. GearSim's carrier landing simulation capability would also be suitable for the design and analysis of landing gear and arrested landing subsystems.

II. GearSim: Landing Gear and Ground Loads Predictive Analysis

GearSim combines a high fidelity, nonlinear 6-DOF landing gear system modeling tool with variable fidelity aeroelastic and flight control system simulation tools, in order to produce an efficient and accurate integrated simulation. Specifically, a Nastran generated linear aeroelastic model can be imported into GearSim for simpler problems, and GearSim can be coupled with nonlinear FE/CFD aeroelastic simulation tools for highly complex, nonlinear, time-varying problems. GearSim's dynamic loads analysis capability has been recently demonstrated by Richards et al. (Ref. [2]).

GearSim is based in MATLAB/Simulink and includes a professional-quality graphical user interface (GUI). The dynamic equations of the landing gear subsystems, such as the leg structure, oleo/pneumatic shock absorber, steering, and braking systems, are modularized in Simulink library blocks. Subsystems are defined by engineering parameters readily available from the relevant drawings and specifications. The GUI consists of a series of menus that guide the user through the landing gear configuration and definition of all relevant subsystems, and then an integrated GearSim model is automatically generated using the library of subsystem models.

A screenshot of the GUI interface is provided in Fig. 1. The subsystem parameters are defined through customized menus. The simulation can be run and post-processed within the GUI, providing relevant loads and stability results at the click of a button. Typical model run times are approximately one to two minutes on an average computer. Batch processing of simulations is available for trade studies and loads cases.

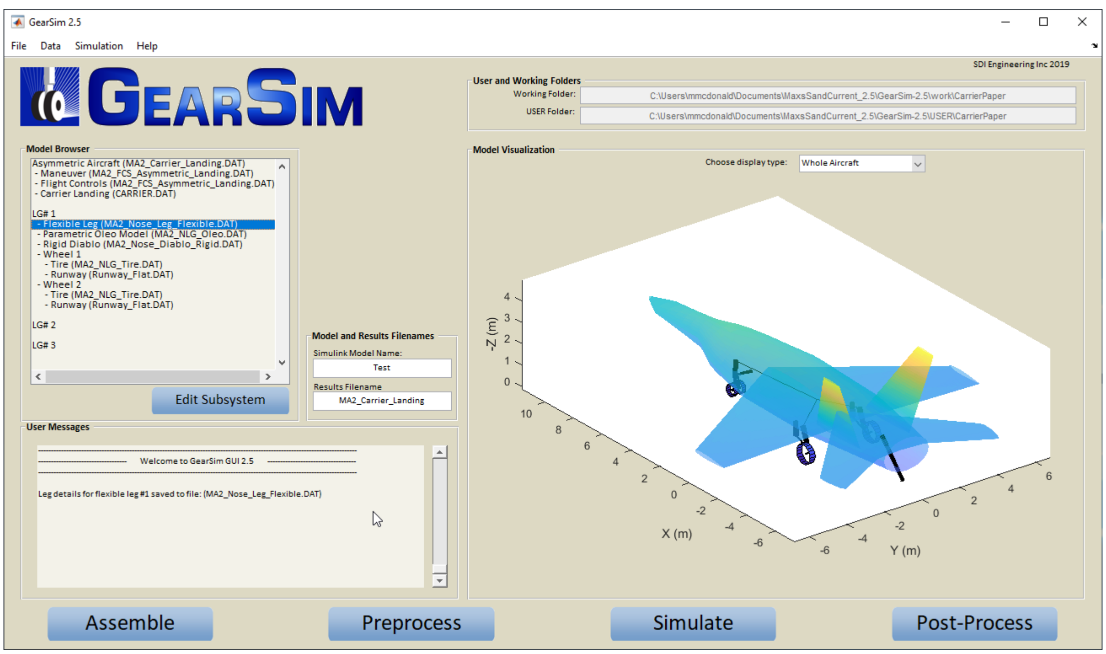

Fig. 1 GearSim user interface

The aircraft can be represented by either a rigid or aeroelastic model. The rigid aircraft model includes 6-DOF flight dynamics, with the option to conduct symmetric (3-DOF) analyses. The aircraft model includes a pitch control system to maintain trim and perform the aircraft de-rotation maneuver after landing, and a lateral/directional control system to maintain lateral trim and perform any lateral maneuvers, such as in a crosswind landing. The initial conditions of the aircraft are determined by a trim calculation feature built into GearSim so that the aircraft begins at a steady flight condition at a prescribed total velocity and descent rate. The pitch attitude, angle of attack, thrust, and elevator settings are determined by the trimming routine in the symmetric case, and in the full 6-DOF case the trim routine also determines the sideslip angle, rudder/aileron deflection, and asymmetric thrust setting.

Improvements to GearSim now allow for carrier landing simulations to be run using the GearSim GUI. In order to integrate the carrier landing capability into GearSim, a deck motion model, an arresting gear system, and a new aircraft model with an attached tail hook were developed.

III. Carrier Deck Motion

Carrier deck motion data was obtained from simulations run during the office of Naval research (ONR)-sponsored project "Systematic Characterization of the Naval Environment (SCONE)" (Ref. [3]). Data is provided for simulated deck motion using a state-of-the-art non-linear seaworthiness prediction code from the Large Amplitude Motions Program (LAMP). This data gives the Cartesian coordinates of a given reference point on the carrier deck with respect to a fixed global origin and the orientation of the deck parameterized in a 1-2-3 Euler angle rotation sequence for each time step of the LAMP code.

A MATLAB script was written to import data files produced from the LAMP code and generate a time history of the deck position and orientation for use with GearSim. Using the deck dimensions, the script produces a rectangle with vertex position vectors relative to the deck reference point. The flight deck reference points are located at the centerline of the landing path at a central point within the arresting wire arrangement and at the stern of the ship. The Euler angles are then converted into a direction cosine matrix (DCM), and the vertex position vectors are rotated via DCM matrix multiplication and then displaced using the Cartesian position vector of the deck reference point. This process is computed for each time step resulting in a time history of the four vertices of the carrier deck.

This data is then implemented into GearSim to produce a 6-DOF carrier deck by using an interpolation scheme to match the frame rate of the GearSim simulation and also to provide deck height and deck angle beneath each landing gear contact point. This process assumes a perfectly flat carrier deck; if the deck geometry and surface conditions are known, deck features such as bumps or slick zones could be implemented into the carrier deck environment via the same coordinate transformation process.

An example of carrier motion data that can be used in a carrier landing simulation is shown in Fig. 2 in which the carrier travels forward at 5 m/s while pitching, rolling, and heaving. The SCONE data includes 60 different cases for six different deck motion conditions with amplitudes of motion that are characterized as 'low', 'moderate', and 'high' with respect to roll attitude and heave rate, so a wide variety of different carrier maneuvers can be simulated. GearSim users select which portion of the carrier motion data is to be used with each carrier landing simulation.

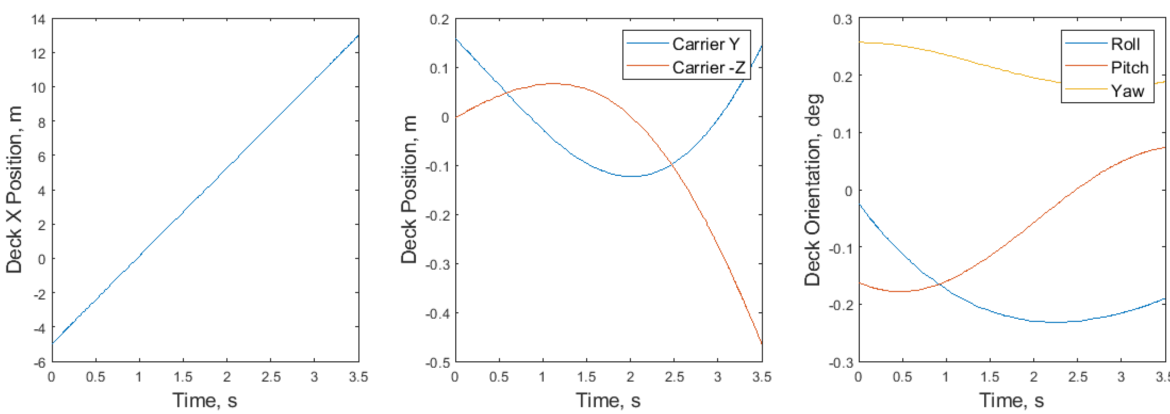

a) b) c)

Fig. 2 Sample SCONE carrier deck motion used in GearSim: a) x-position b) y and -z positions c) roll, pitch and yaw orientation

IV. Arrested Landing System

GearSim's arresting system model was derived from a stand-alone model produced by existing papers, Refs. [4], [5], U.S. Air Force reports, Ref. [6], and a U.S. Navy instruction manual, Ref. [7], for the Mark 7 aircraft arresting system that is standard on many modern aircraft carriers. After developing and testing the arresting model, this feature was fully integrated with the aircraft landing capabilities of GearSim. A diagram of the arresting model integrated into GearSim is shown in Fig. 3.

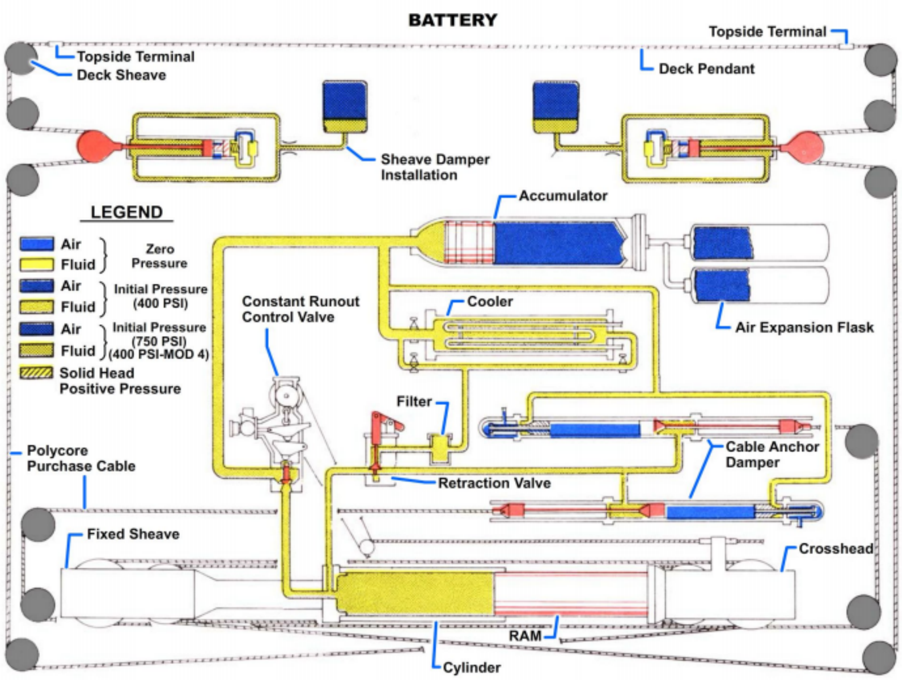

Fig. 3 Mark 7 Mod 3 arresting gear system drawing (Ref. [7])

First, the cable runout and aircraft runout were related mathematically to the deck and cable geometry. The cable runout alters the valve seat height of the constant runout control valve shown in Fig. 3. The constant runout control valve is conical, so the area of the channel that the ram cylinder fluid passes through changes as a trigonometric function of valve cone angle and valve seat height (Ref. [8]). The ram fluid builds up in the accumulator, which then compresses a gas in the accumulator chamber. It was assumed due to the cooling system in the arresting gear and insulation of the accumulator chamber that the compression of this gas is adiabatic, so adiabatic associations relate the stroke of the accumulator to the accumulator pressure. The force on the ram then related to the accumulator pressure, accumulator membrane area, constant runout control valve area and ram head area. This force is then divided by the number of sheaves in the ram crosshead and the number of chords in the arresting cable to calculate the tension generated after the cable is hooked by the aircraft tail hook. Finally, the deck, cable and tail hook geometry can be used to calculate the direction of the resultant force from the cables.

Equations and assumed constants were omitted from this system description for brevity. Refer to Ref. [4] for the full derivation of the arresting gear model.

The arresting gear model implemented into GearSim produced aircraft runout distances and arresting times similar to those seen in Refs. [4], [5] and are consistent with measurements made from arrested landing videos. A side-by-side comparison of simulation results from the GearSim model (Fig. 4a) and the model developed in Ref. [4] (Fig. 4b) is presented below. A comparison of the velocity, position, and hook force plots show that the models have almost identical shapes and exhibit similar behavior. However, it is important to note that small discrepancies are present in runout distance, hook force, and arresting time. These differences are likely due to the fact that the arresting hook simulations in GearSim model the full F-18 aircraft, complete with flight controls, landing gear dynamics, and tire friction models. As such, there are more complex interactions between the aircraft, carrier, and arresting hook in the GearSim model than in the standalone model developed in Ref. [4]. These interactions lead to GearSim's arresting gear exhibiting similar but not identical behavior when compared to the model it was derived from.

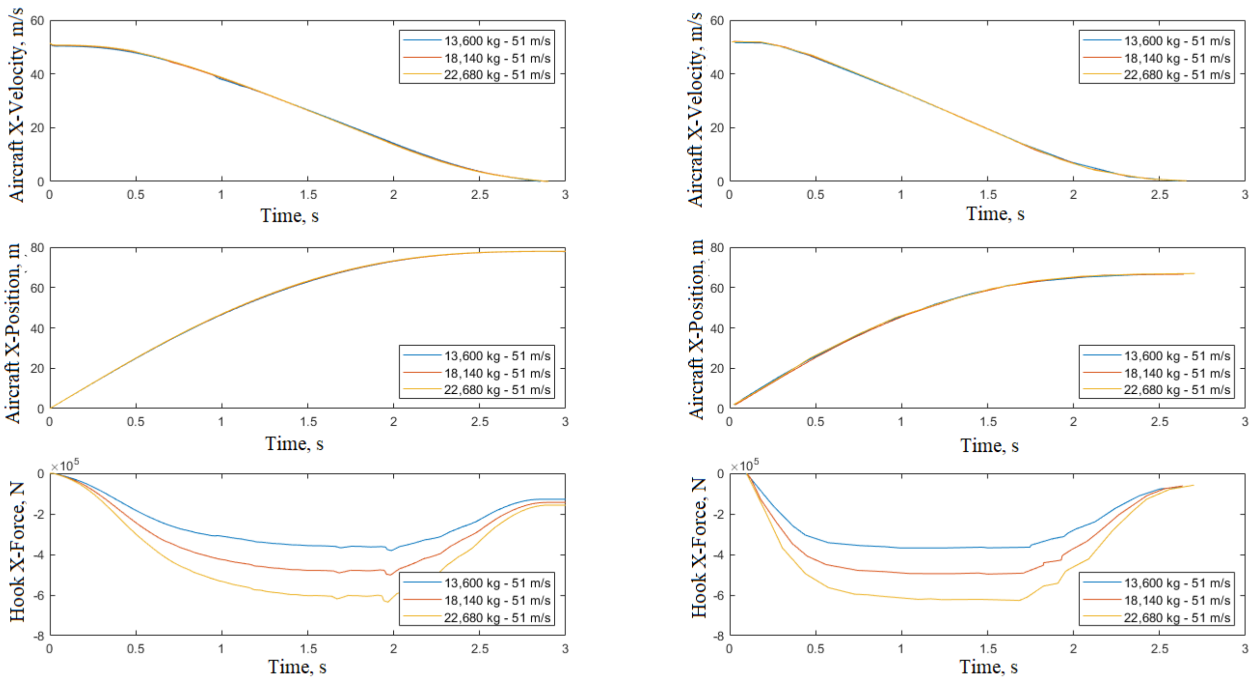

a) b)

Fig. 4 Aircraft velocity, position, and hook force with varying landing mass for (a) GearSim arresting gear system (b) arresting gear system developed in Ref. [4]

Another series of comparison simulations was performed by holding the mass of the aircraft constant and simulating an arrested landing at varying speeds. Again, strong agreement in the response of the arrested aircraft was found between the GearSim and academic models. This validation exercise demonstrates that an effective arresting gear model was developed and supports its use for simulating a full aircraft carrier landing.

V. F/A-18E/F Aircraft Model

One of the challenges in detailed modeling of landing gear systems is the availability of relevant information for the subsystem models. GearSim includes a library of landing gear types and simple design routines that can guide the user towards choosing the appropriate modeling parameters for each landing gear. For carrier landing scenarios, a new model based on the F/A-18E/F Super Hornet (F-18) was developed and implemented into GearSim. The representative aircraft defined in this section is based information obtained from the public domain. This model is not intended as an exact model the F-18, but only a representative model that has been used to analyze the general behavior of this class of aircraft.

A. Aircraft Characteristics and Landing Gear Layout

Weight and geometric information for the representative aircraft were obtained using Ref. [9]. A generic 3-view of an F-18 was used to estimate the mean aerodynamic chord location of the wing; the center of gravity (CG) of the aircraft was assumed to be at the quarter-chord of the mean aerodynamic chord. This technique was also used to estimate the position of the nose and main landing gears (NLG and MLG) with respect to the CG. The maximum landing weight, CG location, and relative locations of the main and nose landing gears were used in a static force balance to determine the static load on the main and nose landing gears. The aircraft weight, overall geometry, and landing gear layout information are given in Table 1. Note that a rigid aircraft was used for this study, as no suitable flexible aircraft model for the F-18 was available.

Table 1 Geometry and weight information

Input	Value
Wing area (m^2)	46.5
Span (m)	13.1
Empty weight (kg)	14,300
Distance from CG to ground (m)	4.0
MLW (kg)	29,900
Mean aerodynamic chord (m)	3.26

Input	Value
Lateral separation of MLG (m)	3.32
Longitudinal distance from NLG to MLG (m)	5.94
Longitudinal distance from MLG to CG (m)	0.74
Longitudinal distance from NLG to CG (m)	5.2
Static load on NLG (N)	73,000
Static load on MLG (per strut) (N)	107,300

B. Tire Model

There are a variety of tire modeling options in GearSim. The tire model used for this study utilizes a spring and damper system to represent the vertical tire response and a table lookup to calculate the longitudinal and lateral friction forces.

According to Ref. [10], the nose landing gear for this aircraft uses 22x6.6-10 tires, and the main landing gears use 30x11.5-14.5 tires. The tire naming convention is *D* x *W-R*, where *D* is the tire diameter, *W* is the tire width and *R* is the wheel rim diameter in inches. Additional data for these tires is summarized in Table 2. The vertical stiffness in Table 2 was calculated by dividing the rated load by the static loaded deflection.

Table 2 Properties for NLG and MLG tires (Ref. [10])

Property	NLG Tire	MLG Tire
Tire Part No.	461B-2515-TL	461B-3204-TL
Tire Diameter (m)	0.558	0.762
Tire Width (m)	0.168	0.292
Rated Load (N)	52,800	110,000
Static Loaded Deflection (m)	0.042	0.064
Vertical Stiffness (N/m)	1.257×10^6	1.719×10^6
Tire Mass (kg)	10.0	20.0
Tire Inertia (kg m^2)	10.8	20.0

The lateral force on the tire and restoring (vertical) moment are considered to be functions of the slip angle and slip ratio. Lookup tables are used to find the longitudinal friction coefficient based on the slip ratio, the lateral friction coefficient based on the slip angle, and the restoring moment arm based on the slip angle.

C. Landing Gear Leg Model

The landing gear leg model can be treated as either rigid or flexible. In the rigid case, the leg model simply transfers forces and moments from the wheel assembly to the aircraft. In the flexible case, a finite element model is constructed for the leg. Reference [11] contains a diagram including a representative NLG and MLG, and this is shown in Fig. 5.

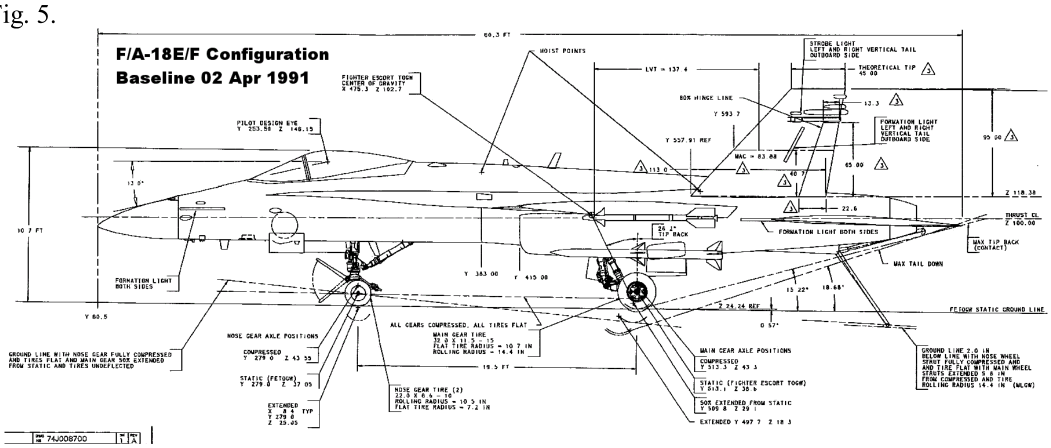

Fig. 5 Diagram of F-18 NLG and MLG used to find leg dimensions (Ref. [11])

Unlike many conventional aircraft, the F-18 utilizes a levered main landing gear system. To account for this, new levered models were developed in GearSim to accurately model the two MLG legs. The landing gear models are presented in Fig. 6.

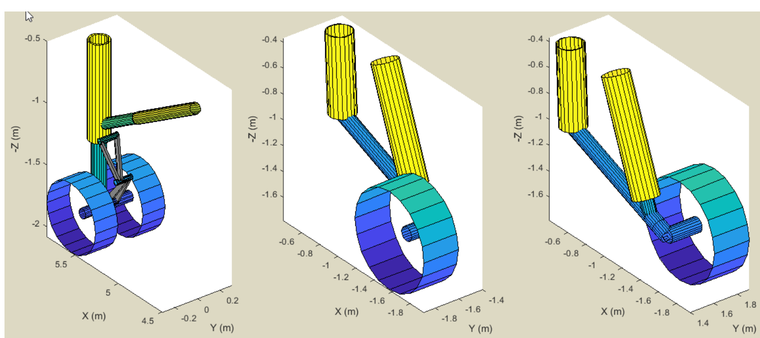

a) b) c)

Fig. 6 GearSim models of F-18 nose (a), port (b), and starboard landing gear (c)

The overall dimensions of the landing gear are presented in Table 3. Note the measurements provided are only a portion of the inputs required for the leg and wheel assembly model definition; the additional inputs are omitted for brevity. For this study, a rigid leg model was used for all landing gear.

Table 3 Overall dimensions of NLG and MLG landing gears

Property	NLG	MLG
Upper tube length (m)	0.724	0.742
Upper tube diameter (m)	0.140	0.196
Maximum extension of lower tube (m)	0.559	0.150
Lower tube diameter (m)	0.134	0.191
Diablo lateral separation (m)	0.419	N/A

D. Oleo/Pneumatic Shock Absorber Model

Modern aircraft typically use oleo/pneumatic shock absorber systems (referred in this work as “oleos”) to absorb the kinetic energy of the aircraft on landing and provide a comfortable touchdown. The energy absorbed by the oleo can be calculated by integrating the closure force as a function of travel on compression and subtracting the integral of closure force as a function of travel on recoil.

The oleo model is a nonlinear mass, spring and damper system. The spring force is a nonlinear function of oleo closure and corresponds to compression of the gas chamber in the oleo. The design force and equivalent mass used to estimate the NLG and MLG oleo properties are shown in Table 4.

Table 4 Inputs used to estimate oleo spring and damping force profiles

Oleo Design Parameter	NLG	MLG
Design Force (N)	88,000	88,000
Sprung Mass (kg)	9,000	9,000
P_S / P_E	4	4
P_C / P_S	3	3
Descent Velocity (m/s)	3	3

This procedure typically results in high coefficient values at low and high stroke values. At low stroke values, the spring force is low, so the ideal damping is high and the velocity is low as the system is just starting to compress. At high stroke values, the velocity is low as the system is slowing to a stop at maximum closure before rebound. The high damping values at low stroke values violates the assumption that damping is low during this portion, so the ideal damping curve was modified to account for this.

Note this procedure was only conducted in the absence of data to describe the oleo spring and damping force. In many practical applications, the oleo spring force and damping characteristics can be obtained from the manufacturer's specifications. In this case, the spring and damping characteristics can be entered into GearSim directly.

E. Fully Integrated Model

The carrier landing model was incorporated into GearSim by combining the previously existing landing gear loads and analysis capabilities with the arresting model, 6-DOF carrier deck, and the F-18 model introduced above. Screenshots of the integrated carrier, aircraft and landing gear models are presented below in Fig. 7. The upper left portion of Fig. 7 shows an isometric view of the aircraft and landing gear model at the time of connection with the cable; the lower portion shows a side view of the model just after connection; the upper right portion shows a top view at the end of the simulation, with the aircraft at rest.

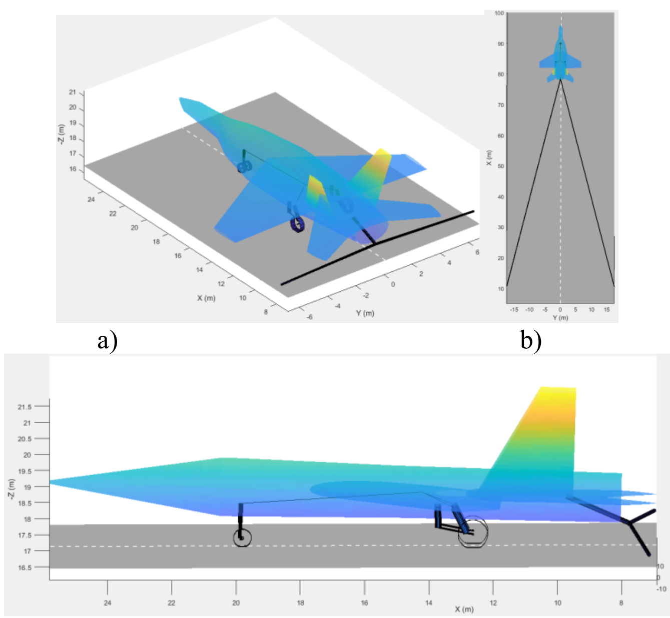

Fig. 7 Simulation screenshots of aircraft, tail hook, carrier and arresting cable

VI. Carrier Landing Simulation

The full arrested carrier landing simulation consists of the F-18 model landing with an initial airspeed of 52 m/s (101 kts), and comes to rest in under 4 seconds. The aircraft begins the simulation with a trimmed descent of 1 m/s at a pitch angle of 2 degrees. The carrier deck motion presented in Fig. 2 was used for this simulation. After the MLG touches down, a de-rotation command is prescribed to the pitch attitude control system to bring the nose gear into contact with the deck, and the aircraft tail hook also connects with the arresting cable.

Fig. 8 shows the aircraft's position, velocity and pitch angle during the carrier landing simulation. The velocity decreases from approximately 47 m/s (relative to the carrier deck) to zero in less than four seconds. The aircraft's global *x*-velocity ends at a value of 5 m/s, which equals the carrier's forward velocity, since the aircraft is no longer moving relative to the carrier. The aircraft's vertical position approaches the same value as the carrier deck while the aircraft's pitch angle tends towards zero degrees, which shows that the aircraft made a level landing on the carrier deck. The difference between the aircraft *z*-position and the carrier *z*-position at the end of the simulation is a result of the landing gear geometry.

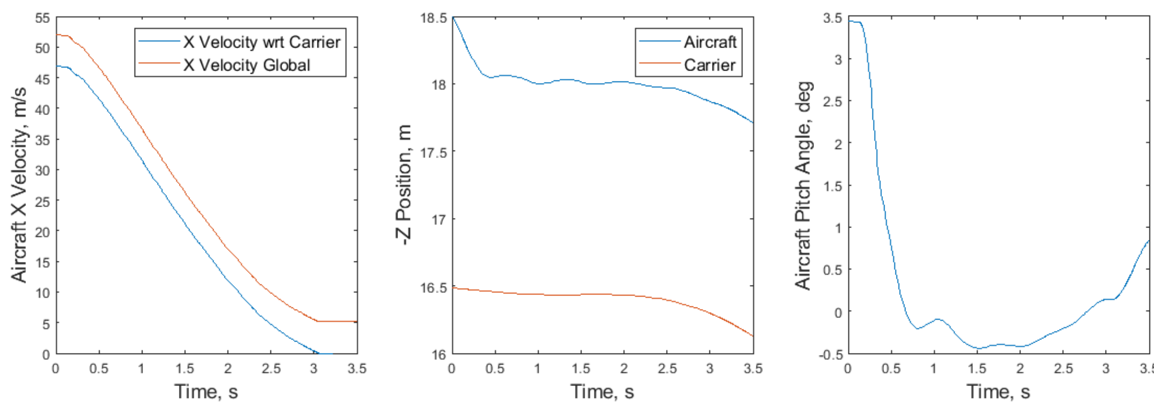

a) b) c)

Fig. 8 Aircraft velocity (a), aircraft/carrier position (b), and aircraft pitch angle (c)

The tire and oleo deflections for the starboard MLG during the carrier landing simulation are shown in Fig. 9. Both the tire deflection and oleo closure reach a steady value a few seconds after contacting the ground, indicating the aircraft has stabilized after touchdown.

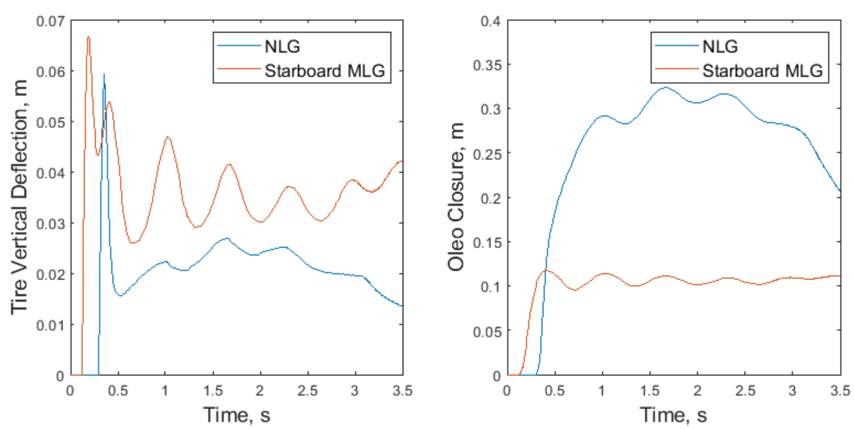

a) b)

Fig. 9 Starboard MLG vertical tire deflection (a) and oleo closure (b)

The arresting hook force and the leg forces in the vertical and longitudinal directions of the NLG and starboard MLG are shown in Fig. 10. The lateral forces on the landing gear are nonzero due to the carrier deck motion, but are orders of magnitude smaller than the vertical and longitudinal forces. The arresting system is designed to turn off once the aircraft's velocity reaches zero, and this behavior is demonstrated in Fig. 10a. The NLG contact occurs after the MLG contact as the pitch angle of the aircraft is reduced.

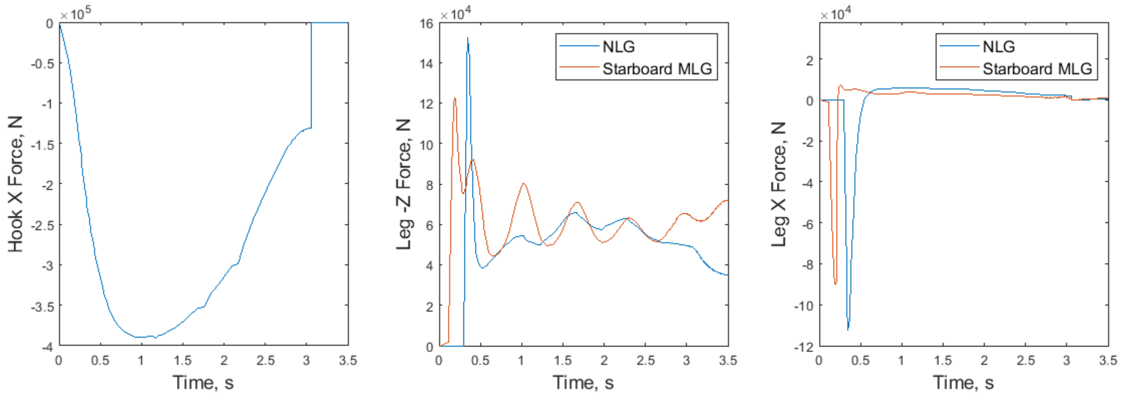

a) b) c)

Fig. 10 Forces on arresting hook (a) and landing gear legs (b, c)

The loads in Fig. 10 were compared to the loads for a conventional runway landing using the same F-18 model. The carrier landing resulted in much higher loads on the NLG, due to the strong pitch-down moment created by the large hook force, which acts in the x-direction below the aircraft CG. The carrier motion resulted in lateral loads on all landing gear on the order of 1 kN. The x- and z- loads on the MLG were similar for the two cases. This comparison indicates that the main effect of the carrier landing on the landing loads is a significant increase in the nose landing gear loads due to the strong pitch-down moment.

VII. Conclusion

This paper introduces GearSim as a tool that is ideal for analyzing the landing gear loads and dynamic response of arrested carrier landings. Simulation results for a carrier landing simulation are presented as an example of GearSim's capability.

The results produced by GearSim have a wide variety of practical applications to carrier operations. The aircraft certification process requires a significant number of flight and ground tests to ensure the aircraft's structure and landing gear perform safely under a wide range of operations. A reduction of the required number of test points in flight and ground tests could save significant cost and time during the design and analysis process, and can be achieved by using a reliable and accurate simulation capability. Simulation results from GearSim could also be integrated into a flight simulator to improve the accuracy and pilot experience of performing an arrested landing on an aircraft carrier under a wide variety of conditions. This could make flight simulators more effective for training pilots and provide more accurate simulations of many different landing scenarios before they attempt their first real carrier landing. Furthermore, carrier landing simulations can improve prediction and understanding of extreme or difficult to obtain flight test cases such as strong crosswinds, variable runway conditions, hard landings, and abrupt maneuvers.

Acknowledgments

SDI Engineering would like to thank the Landing Gear Test Facility located at Wright Patterson Airforce Base in Dayton, OH for their support of the GearSim development and validation effort through the Small Business Initiative Research program. This material is based upon work supported by the United States Air Force under contract award FA2487-16-C-0085 to SDI Engineering Inc. Any opinions, findings, and conclusions or recommendations expressed in this publication are those of the author(s) and do not necessarily reflect the views of the United States Air Force or SDI Engineering Inc. The authors would also like to thank Ryan Wallace for his assistance in initial research and model development.

Disclaimer: "This report was prepared as an account of work sponsored by an agency of the United States Government. Neither the United States Government nor any agency thereof, nor any of their employees, makes any warranty, express or implied, or assumes any legal liability or responsibility for the accuracy, completeness, or

usefulness of any information, apparatus, product, or process disclosed, or represents that its use would not infringe privately owned rights. Reference herein to any specific commercial product, process, or service by trade name, trademark, manufacturer, or otherwise does not necessarily constitute or imply its endorsement, recommendation, or favoring by the United States Government or any agency thereof. The views and opinions of authors expressed herein do not necessarily state or reflect those of the United States Government or any agency thereof."

References

[1] Currey, N. S., *Aircraft Landing Gear Design, Principles and Practices*. American Institute of Aeronautics and Astronautics, Inc. 1988.

[2] Richards, P. W., and Erickson, A., "Dynamic Ground Loads Analysis Using Detailed Modeling of Landing Gear and Aircraft Modeling," *AIAA SciTech 2019 Forum*, Jan. 2019.

[3] Schwartz, A., "SCONE - Standard Deck Motion Data for a Generic Carrier (CVN)," *Office of Naval Research*, Jun. 2016.

[4] Lv, K., Zhu, Q., and Li, X., *Modeling and Simulation for Arrested Landing of Carrier-based Aircraft.* Proceedings of the 2011 IEEE International Conference on Mechatronics and Automation. 2011

[5] Shen, W., Zhao, Z., Ren, G., and Liu, J., *Modeling and Simulation of Arresting Gear System with Multibody Dynamic Approach*. Mathematical Problems in Engineering. 2013

[6] Michael F. Louise. A Study of the effect of different Cam Designs on Mark7 Mod1 Arresting Gear Performance, AD-A061486, August 1978.

[7] *Chapter 4: MARK (MK) 7 AIRCRAFT RECOVERY EQUIPMENT*. U.S. Navy BMR Study Material.

[8] Cunxing. He, Hydraulic Component, Beijing: China Machine Press, 1982, pp. 439-447.

[9] "F/A-18E/F 'Super Hornet'," *FAS Military Analysis Network.* URL: https://fas.org/man/dod-101/sys/ac/f-18.htm. [Last updated November 2016; accessed November 2019]

[10] Goodyear Aviation, "Global Aviation Tires," Aircraft Tire Databook. URL: https://www.aps-aviation.com/wp-content/uploads/goodyear-aircarft-tire-data.pdf [effective date October 2002, retrieved November 2019].

[11] "F/A-18 E/F Baseline Configuration," *F-16.net.* URL: http://www.f-16.net/forum/download/file.php?id=23759&sid=a1519cec2a2eb40afc1b70b202eddc09&mode=view. [accessed November 2019]